



1    **Part 2: Quantitative contributions of cyanobacterial alkaline phosphatases to biogeochemical  
2    rates in the subtropical North Atlantic**

3    *Noelle A. Held<sup>1,2,3</sup> \*, \*\*, Korrina Kunde<sup>4,5</sup> \*\*, Clare E. Davis<sup>6</sup> †, Neil J. Wyatt<sup>5</sup>, Elizabeth L. Mann<sup>7</sup>, E.  
4    Malcolm. S. Woodward<sup>8</sup>, Matthew McIlvin<sup>1</sup>, Alessandro Tagliabue<sup>6</sup>, Benjamin S. Twining<sup>8</sup>, Claire  
5    Mahaffey<sup>6</sup>, Mak Saito<sup>1</sup>, Maeve C. Lohan<sup>5</sup>*

6

7    <sup>1</sup>Department of Marine Chemistry and Geochemistry, Woods Hole Oceanographic Institution, Woods Hole,  
8    USA

9    <sup>2</sup>Department of Environmental Systems Science, ETH Zürich, Zürich, Switzerland

10    <sup>3</sup>Department of Biological Sciences, Marine and Environmental Biology Section, University of Southern  
11    California, Los Angeles, CA, USA

12    <sup>4</sup>School of Oceanography, University of Washington, Seattle, USA

13    <sup>5</sup>Ocean and Earth Sciences, National Oceanography Centre, University of Southampton, Southampton, UK

14    <sup>6</sup>Department of Earth, Ocean, and Ecological Sciences, University of Liverpool, Liverpool, UK

15    <sup>7</sup>Bigelow Laboratory for Ocean Sciences, East Boothbay, USA

16    <sup>8</sup>Plymouth Marine Laboratory, Plymouth, UK

17

18    \*Corresponding author: N.A. Held (nheld@usc.edu)

19    \*\*These authors contributed equally

20    <sup>†</sup>now at: Springer Nature, London, UK

21    **Abstract**

22    Microbial enzymes alter marine biogeochemical cycles by catalyzing chemical transformations that  
23    bring elements into and out of particulate organic pools. These processes are often studied through  
24    enzyme rate-based estimates and nutrient-amendment bioassays, but these approaches are limited in  
25    their ability to resolve species-level contributions to enzymatic rates. Molecular methods including  
26    proteomics have the potential to link the contributions of specific populations to the overall  
27    community enzymatic rate; this is important because organisms will have distinct enzyme  
28    characteristics, feedbacks, and responses to perturbations. Integrating molecular methods with rate  
29    measurements can be achieved quantitatively through absolute quantitative proteomics. Here, we use  
30    the subtropical North Atlantic as a model system to probe how absolute quantitative proteomics can  
31    provide a more comprehensive understanding of nutrient limitation in marine environments. The  
32    experimental system is characterized by phosphorus stress and potential metal-phosphorus co-  
33    limitation due to dependence of the organic phosphorus scavenging enzyme alkaline phosphatase on  
34    metal cofactors. We performed nutrient amendment incubation experiments to investigate how  
35    alkaline phosphatase abundance and activity is affected by trace metal additions. We show that the  
36    two most abundant picocyanobacteria, *Prochlorococcus* and *Synechococcus* are minor contributors to



37 total alkaline phosphatase activity as assessed by a widely used enzyme assay. This was true even  
38 when trace metals were added, despite both species having the genetic potential to utilize both the Fe  
39 and Zn containing enzymes, PhoX and PhoA respectively. Serendipitously, we also found that the  
40 alkaline phosphatases responded to cobalt additions suggesting possible substitution of the metal  
41 center by Co in natural populations of *Prochlorococcus* (substitution for Fe in PhoX) and  
42 *Synechococcus* (substitution for Zn in PhoA). This integrated approach allows for a nuanced  
43 interpretation of how nutrient limitation affects marine biogeochemical cycles and highlights the  
44 benefit of building quantitative connections between rate and “-omics” based measurements.

45



## 46 Introduction

47 Microbial enzymes alter marine biogeochemical cycles by catalysing chemical transformations and  
48 facilitating the movement of elements through planetary reservoirs. On one hand, enzyme  
49 contributions from different groups of microbes can be considered collectively, for instance in rate-  
50 based or bioassay incubation experiments where the activities of the entire microbial community are  
51 aggregated. On the other hand, we anticipate that the enzymes of different organisms will have  
52 different activities and responses to perturbations; this means that resolving enzyme provenance could  
53 enhance the quantitative connection between microbial activity and biogeochemical rates (e.g. the  
54 goals of the fledgling Biogeoscapes program (Saito et al., 2024)). “-Omics” based methods,  
55 particularly proteomics which directly resolves protein/enzyme concentrations, can provide a window  
56 into the relationships between microbial abundance, enzyme concentration, and biogeochemical rates.

57 In this work we use quantitative proteomics to constrain the relative contributions of different  
58 microbes (*Synechococcus* and *Prochlorococcus*) to biogeochemical rates of alkaline phosphatase  
59 activity in the oligotrophic subtropical North Atlantic gyre. In this region, primary production is  
60 constrained by availability of dissolved inorganic nitrogen (DIN) and phosphorus (DIP), but inputs of  
61 atmospherically derived iron (Fe) from Saharan desert dust create a niche for nitrogen fixation,  
62 partially alleviating nitrogen limitation but driving the system to DIP depletion (Martiny et al., 2019;  
63 Moore et al., 2013). Lack of DIP then drives a shift towards the acquisition of the abundant yet less  
64 bioavailable dissolved organic phosphorus (DOP) by phytoplankton (Lomas et al., 2010; Mather et al.,  
65 2008). The DOP pool includes relatively labile phosphomono- and diesters (together ~75 to 85 % of  
66 DOP) that derive from ribonucleic acids, adenosine phosphates and phospholipids (Kolowith et al.,  
67 2001; Young and Ingall, 2010). These compounds cannot be directly assimilated but require the  
68 phosphate group to be cleaved from the ester moiety first. Cleaving is catalysed by a range of  
69 hydrolytic enzymes, such as alkaline phosphatases, which are common in marine microbes, including  
70 bacterial as well as eukaryotic phytoplankton (Dyrhman and Ruttenberg, 2006; Luo et al., 2009;  
71 Shaked et al., 2006). Reflecting this, alkaline phosphatase activity (APA) is high across the  
72 oligotrophic gyres (Browning et al., 2017; Davis et al., 2019; Duhamel et al., 2010; Mahaffey et al.,  
73 2014; Wurl et al., 2013).

74 Alkaline phosphatase activity is commonly regulated by intracellular phosphate levels  
75 (Santos-Benito, 2015) and appears to be closely linked to low ambient DIP concentrations (Mahaffey  
76 et al., 2014). However, these enzymes also have a metal dependence, as metal co-factors are involved  
77 in the hydrolysis process at the active site. Different alkaline phosphatases exist that, while sharing  
78 function, evolved independently and have distinct metal requirements. For example, in *Escherichia*  
79 *coli* (*E. coli*) the alkaline phosphatase PhoA has two Zn<sup>2+</sup> (zinc) or Co<sup>2+</sup> (cobalt) ions and one Mg<sup>2+</sup>  
80 (magnesium) ion at each active site per homodimer (Coleman, 1992), and in *Pseudomonas fluorescens*



81 the monomeric alkaline phosphatase PhoX has two  $\text{Fe}^{3+}$  ions and three  $\text{Ca}^{3+}$  (calcium) ions(Yong et  
82 al., 2014). The active sites of PhoA and PhoX in marine microbes have yet to be characterized but  
83 based on sequence homology are presumed to be like these model organisms, leading to the  
84 hypothesis that alkaline phosphatase activity to be limited by scarce Fe, Zn, or Co trace metals in the  
85 marine environment (Lohan and Tagliabue, 2018).

86 Global change is predicted to intensify phosphorus stress and alter trace metal and nutrient  
87 cycles in the ocean (Hoffmann et al., 2012; Kim et al., 2014). Throughout the North Atlantic, the  
88 utilisation of DOP is widespread (Mather et al., 2008) and whole community rates of APA are high  
89 compared with other oceanic regions (Duhamel et al., 2010; Mahaffey et al., 2014). At this time, it is  
90 not known which microbes and enzyme types are responsible for bulk APA in the North Atlantic and  
91 elsewhere. Resolving this could lead to a more quantitative understanding of how APA activity is  
92 regulated in the modern ocean, allowing better predictions of future changes in enzyme abundance  
93 and activity and the resulting influence on carbon export. In this study, we use field-based quantitative  
94 proteomics to develop an inventory of alkaline phosphatase activity and to identify nutrient-related  
95 regulatory controls on alkaline phosphatase that are distinct for different organisms. We use this as a  
96 proof of concept for developing quantitative connections between biogeochemical rates and “-omics”  
97 based measurements of microbial enzymes, a topic that is of interest to ongoing international efforts  
98 to characterize ocean metabolism.

## 99 Methods

### 100 Shipboard bioassays

101 All samples for this study were collected on board the *RRS James Cook* during research cruise JC150  
102 (GEOTRACES process study GApr08), on a zonal transect at 22 °N leaving Guadeloupe on June 26<sup>th</sup>  
103 and arriving in Tenerife on August 12<sup>th</sup>, 2017, with multiple stations occupied for bioassays. A  
104 detailed description of the bioassays and analysis of environmental parameters is presented in  
105 Mahaffey et al. (submitted as a companion to this article).

106 Briefly, surface seawater was collected and processed according to trace metal clean protocols  
107 and before dawn. For each location, duplicate or triplicate 24 L polycarbonate (Nalgene) carboys were  
108 filled and spiked with additions of Fe, Zn or Co, as detailed in Table 1. The seawater was incubated at  
109 ambient sea surface temperature and 50 % surface light level for 48 h from dawn to dawn with a  
110 12:12 h simulated light cycle using white daylight LED panels.

111 *Table 1 Bioassay details at each station, showing the types of treatments, the amount of metal added, and the number of*  
112 *replicates per treatment for which proteomics analyses were conducted. Note that one of the three replicates of the Fe*  
113 *addition at the Station at 31 °W (\*) was removed as an outlier from all further analysis.*

	Station at 54 °W	Station at 50 °W	Station at 45 °W	Station at 31 °W
--	------------------	------------------	------------------	------------------



Treatment	Control	-	-	-	-
Fe	+ 1.0 nM				
Zn	+ 1.0 nM	+ 1.0 nM	+ 0.5 nM	+ 1.0 nM	
Co	+ 50 pM	+ 50 pM	+ 50 pM	+ 20 pM	
<b>Replicates per treatment</b>		2	2	2	3*

114 After the incubation period, subsamples for proteins were collected into acid cleaned 10 L  
115 polycarbonate carboys (Nalgene) and immediately filtered, collecting the >0.22 µm fraction on  
116 polyethersulfone membrane filter cartridges (Millipore, Sterivex) and recording the filtered volume.  
117 Any remaining water was pressed out with an air-filled syringe, the filtration unit was sealed with clay  
118 and then frozen at -80 °C. This procedure was repeated for the second (and third where applicable)  
119 replicate of each treatment.

## 120 **Protein extraction and digestion**

121 All plastics materials were washed with ethanol and dried before usage. All samples from one station  
122 were processed together in one extraction and digestion cycle. The frozen Sterivex filter cartridges  
123 were transported to the laboratory on ice and cut open with a tube cutter. The filters were cut out from  
124 their holders with razor blades and placed into 2 ml microfuge tubes (Eppendorf). Following  
125 previously established protocols(Held et al., 2020; Saito et al., 2014)Click or tap here to enter text.,  
126 proteins were extracted in a 1 % sodium dodecyl sulfate (SDS) buffer for 15 min at 20 °C, followed  
127 by 10 min at 95 °C for denaturation, and 1 h at 20 °C while shaking at 350 rpm. The protein extract  
128 was then centrifuged at 13.5 rpm for 20 min, with the impurities-free supernatant collected and then  
129 spin-concentrated for 1 h in 5 kD membrane filters (Vivaspin, GE Healthcare). Total protein  
130 concentrations were then measured by bicinchoninic assay (BCA) (Pierce) on a Nanodrop ND-1000  
131 spectrophotometer (ThermoScientific). Proteins were left to precipitate in a 50:50 solvent mixture of  
132 methanol and acetone (Fisher) with 0.004 % concentrated HCl (Sigma, ACS 37 %) for 5 days at -20  
133 °C. At the end of the precipitation period, samples were centrifuged at 13.5 rpm at 4 °C, supernatants  
134 were removed, and the remaining protein pellets were vacuum-dried (DNA110 Savan SpeedVac,  
135 ThermoFisher). Pellets were redissolved in 50 µl SDS buffer, and the post-precipitation total protein  
136 concentrations were measured via a second BCA assay to assess recovery. The protein extracts were  
137 digested with the proteolytic enzyme trypsin (1 µg per 20 µg protein; Promega #V5280) in a  
138 polyacrylamide tube gel(Lu and Zhu, 2005). The digested samples were concentrated by vacuum  
139 drying and stored at -20 °C until analysis. The final volume was recorded to calculate the total protein  
140 concentration in the processed sample, typically ~1 µg µl<sup>-1</sup>.

## 141 **Target protein selection**



142 Protein biomarkers for *Synechococcus* and *Prochlorococcus* were chosen to detect DIP stress (PstS)  
143 and related coping mechanisms via DOP hydrolysis (PhoA and PhoX) in our samples (Table 2). PstS  
144 is the substrate-binding protein of the high-affinity phosphate ABC (ATP-Binding Cassette)  
145 transporter, which is upregulated under low intracellular phosphate concentrations via the *pho* regulon  
146 and has previously been used as an indicator of DIP stress (Cox and Saito, 2013; Martiny et al., 2006;  
147 Scanlan et al., 1993). PhoA and PhoX are the Zn/Co-dependent and Fe-dependent alkaline  
148 phosphatases, respectively, which facilitate the acquisition of phosphorus from the DOP pool.

149 *Table 2 Details on the quantified peptide biomarkers that are used to represent each protein in the subsequent plots and*  
150 *discussions. For Prochlorococcus strains, 'HL' and 'LL' refer to high-light and low-light adapted strains, respectively.*

Protein		Quantified peptide (amino acid sequence)	Isolate strains with this peptide
<i>Synechococcus</i>	<b>PhoA</b>	HYIAVALER	WH8102 (clade III)
	<b>PhoX</b>	SQAGAELFR	WH8102 (clade III)
	<b>PstS</b>	WFQELAAAGGPK	RCC307 (clade X)
<i>Prochlorococcus</i>	<b>PhoA</b>	IYVIDPSSSPALLER	MIT9311 (clade HL II) MIT9312 (clade HL II) MIT9314 (clade HL II)
	<b>PhoX</b>	GNLWIQTDGK	MIT9314 (clade HL II)
	<b>PstS</b>	LSGAGASFPAK	MIT9301 (clade HL II) MIT9302 (clade HL II) MIT9311 (clade HL II) MIT9312 (clade HL II) MIT9314 (clade HL II) SB (clade HL II) NATL1A (clade LL I) NATL2A (clade LL I)

151

152 The criteria for a peptide of the protein biomarker to be used for quantification were as  
153 follows. Firstly, we attempted to minimise the presence of methionine and cysteines because they are  
154 subject to oxidation and cause modifications of the mass-to-charge ratio (m/z) during the analyses.  
155 Secondly, the specificity and least common ancestor of each tryptic peptide was assessed using  
156 METATRYP (<https://metatryp.whoi.edu/>) (Saunders et al., 2020). It has been demonstrated that  
157 carefully selected tryptic peptides, screened by using tryptic peptides databases made from genome  
158 sequences like METATRYP, can be used to identify specific proteins in mixed microbial assemblages  
159 to the species or even sub-species (ecotype) taxonomic resolution (Saito et al., 2015). Finally, the  
160 performance of each precursor ion was visually inspected in Skyline (MacLean et al., 2010) for peak  
161 shape and signal to noise-ratio during uncalibrated test measurements using a target list containing  
162 many peptides of cyanobacterial alkaline phosphatases on a subset of the incubation samples.

### 163 Isotopically labelled standard peptides

164 The absolute quantitation of the target peptides was achieved using heavy nitrogen isotope-labelled  
165 peptide standards (Saito et al., 2020). Briefly, DNA was synthesized containing the reverse-translated



166 gene sequences for our target peptides interspaced with spacer sequences and ligated with a  
167 PET30a(+) plasmid vector using the BAMHI 5' and XhoI 3' restriction sites (Novagen; obtained  
168 through PriorityGENE, Genewiz). Different nucleotide sequences were used to encode for the spacer  
169 (amino acid sequence: TPELFR) to avoid repetition. As per manufacturer instructions, the plasmid  
170 was suspended in TE buffer (10 mM Tris-HCl, 1 mM ethylenediaminetetraacetic acid) to 10 ng  $\mu$ l<sup>-1</sup>  
171 and of this 1  $\mu$ l was added to 20  $\mu$ l competent Tuner(DE3)pLysS *E. coli* cells on ice. The cells were  
172 heated to 42 °C for 30 sec to initiate transformation, followed by 2 min on ice. At room temperature,  
173 80  $\mu$ l <sup>15</sup>N-enriched (98 %, Cambridge Isotope Laboratories), kanamycin-containing (50  $\mu$ l ml<sup>-1</sup>) SOC  
174 medium was added, and cells were incubated for 30 min at 37 °C at 300 rpm. Subsequently, 25  $\mu$ l  
175 were transferred to pre-heated (37 °C) 50  $\mu$ g ml<sup>-1</sup> agar plates and incubated overnight. One colony was  
176 added to 500  $\mu$ l <sup>15</sup>N-enriched SOC medium containing 50  $\mu$ l ml<sup>-1</sup> kanamycin as a starter culture and  
177 incubated for 3 h at 37 °C at 350 rpm. Next, 200  $\mu$ l of the starter culture were transferred into 50 ml  
178 flat incubation flasks with 10 ml SOC medium and incubated for approximately 3 h at 37 °C and 350  
179 rpm until the optical density at 600 nm reached 0.6. Protein production was induced by the addition of  
180 100 mM isopropyl  $\beta$ -D-1-thiogalactopyranoside to the culture and incubating at 25 °C overnight.  
181 Inclusion bodies were initially harvested using BugBuster protein extraction protocols (Novagen).  
182 The remaining pellet containing the inclusion bodies, i.e. the insoluble protein fraction, was  
183 resuspended in 400  $\mu$ l 6 M urea, left on the shaker table at 350 rpm at room temperature for 3 h, and  
184 then moved to the fridge overnight. The next morning, the proteins were reduced, alkylated, and  
185 digested with trypsin as outlined above for the bioassay samples, and stored frozen at -20 °C until use.

#### 186 **Absolute protein quantitation**

187 To determine the absolute concentration of the peptides in the heavy peptide mixture, commercial  
188 standard peptides of known concentration were used. In addition to the peptides of interest, a range of  
189 tryptic peptide sequences from commercially available standards (apomyoglobin, Sigma; Pierce  
190 Bovine Serum Albumin, ThermoFisher) were included in the original plasmid design. Using these, the  
191 calibrated concentration of the heavy peptide mixture had a relative standard deviation of 57 %, with  
192 the standard deviation resulting from the cross-peptide and cross-replicate variability (n=3) (Fig. S5).  
193 Due to the lack of reference materials, the accuracy of the protein concentrations in our bioassay  
194 samples cannot be assessed. A systematic method-focused study addressing the precision and  
195 accuracy of these measurements as well as the development of reference materials will be essential for  
196 using absolute quantitative proteomics in the marine environment in the future (Saito et al., 2024). The  
197 linear performance range of each heavy peptide standard was assessed using standard curves of the  
198 peptide mixture. Targeted proteomic measurements were made by high pressure liquid  
199 chromatography with tandem mass spectrometry (HPLC-MS/MS) on an Orbitrap Fusion Tribrid Mass  
200 Spectrometer (ThermoFisher). Two  $\mu$ g of each sample diluted to 10  $\mu$ l in buffer B (0.1 % formic acid  
201 in acetonitrile) was spiked with 10 fmol  $\mu$ L<sup>-1</sup> of the heavy peptide mixture and injected into the



202 Dionex nanospray HPLC system at a flow rate of  $0.17 \mu\text{l min}^{-1}$ . The chromatography consisted of a  
203 nonlinear gradient from 5 to 95 % of buffer B with the remaining concentration consisting of buffer A  
204 (0.1 % formic acid in LC-grade  $\text{H}_2\text{O}$ ). Precursor ( $\text{MS}^1$ ) ions were scanned for the  $\text{m/z}$  of the heavy  
205 peptide standards and their natural light counterparts. The mass spectrometer was run in parallel  
206 reaction monitoring mode and only peptides included in the precursor inclusion list were selected for  
207 fragmentation. Absolute peptide concentrations were calculated from the ratio of the peak areas of the  
208 product ions ( $\text{MS}^2$ ) of the heavy peptide of known concentration to the natural light peptide  
209 (calculated in Skyline (MacLean et al., 2010)). Manual validation of peak shapes was performed for  
210 each peptide and sample. Differences between samples with regards to filtration volume, initial  
211 protein mass and recovery after precipitation were accounted for. Final peptide concentrations will  
212 hereafter be used to represent corresponding protein concentrations, with the caveat that the  
213 measurements are not able to discern active versus non-active proteins. The status of metalation and if  
214 the protein is correctly folded or functions as a polymeric complex cannot be determined from this  
215 method.

216 **Significant responses**

217 Changes in protein concentrations in response to metal additions were compared relative to the  
218 unamended control treatment after 48 h. This approach accounts for any bottle effects. Due to the  
219 unique challenges of ocean proteomics sampling and large-scale trace-metal clean bioassays, treatment  
220 replication was limited to  $n = 2$  at  $54^\circ\text{W}$ ,  $50^\circ\text{W}$  and  $45^\circ\text{W}$  and to  $n = 3$  at  $31^\circ\text{W}$ . Many statistical  
221 tests assume normal distributions, which for  $n = 2$  is not assessable. Therefore, in our case, significant  
222 differences in protein concentrations were evaluated using a two-fold change criterion, in which the  
223 concentrations in all replicates of the metal treatments must lie outside a two-fold change in the  
224 average  $\pm$  one standard deviation of the control to be deemed a significant response. The fold-change  
225 in expression and in particular the two-fold change is an accepted and commonly used metric to  
226 identify proteins that are significantly more or less expressed across different conditions (Carvalho et  
227 al., 2008; Lundgren et al., 2010; Zhang et al., 2006).

228 For the biogeochemical parameters measured in the bioassays, i.e. Chl-*a*, APA and cell counts  
229 replication was not limited to  $n=2$  in most cases. Where  $n=3$ , ANOVA ( $\alpha=0.05$ ) followed by Tukey  
230 posthoc tests were applied to compare the Control treatments with other treatments.

231 **Results**

232 **Biogeochemical setting**

233 The oligotrophic subtropical North Atlantic is marked by high deposition of Saharan desert dust,  
234 delivering large amounts of Fe and other lithogenic trace metals to the surface ocean (Kunde et al.,



235 2019). During JC150, contrasting biogeochemical regimes existed in the western and eastern basin  
236 with high-metal, low-phosphorus, low-nitrogen surface waters at the 54 °W and lower-metal, higher-  
237 phosphorus, higher-nitrogen surface waters 31 °W Mahaffey et al. (submitted as a companion to this  
238 article). Furthermore, *Synechococcus* was two-fold more abundant in the west than in the east, whilst  
239 *Prochlorococcus* was more than six-fold more abundant in the east than in the west and numerically  
240 more abundant than *Synechococcus* throughout. Overall, the stations at 50 °W and 45 °W exhibited  
241 biogeochemical intermediates to the conditions in the east and west. The confluence of gradients in  
242 both DIP and trace element availability, as well as clear shifts in microbial community structure,  
243 provide a natural field laboratory to probe how environmental drivers differentially influence the  
244 contributions of dominant microbes to whole-ecosystem enzyme activity.

245 *Table 3 Date, location and biogeochemical conditions at 40 m depth at the start (t<sub>0</sub>) of the bioassays. Biogeochemical*  
246 *parameters are presented as the average ± one standard deviation of replicate t<sub>0</sub> samples, except for the singlet samples of*  
247 *DOP at Station 4 and dCo at all stations. Mixed layer depths (MLD; defined after<sup>52</sup>) averages over multiple days, as these*  
248 *were not always determined on the exact day of bioassay set-up.*

	Parameter	Station at 54 °W	Station at 50 °W	Station at 45 °W	Station at 31 °W
General	Date	11 <sup>th</sup> July 2017	15 <sup>th</sup> July 2017	19 <sup>th</sup> July 2017	5 <sup>th</sup> August 2017
	Location	22 °N 54 °W	22 °N 50 °W	23 °N 45 °W	22 °N 31 °W
	SST (°C)	27	27	26	25
	MLD (m)	24 ± 3 (5 <sup>th</sup> to 8 <sup>th</sup> July)	33 ± 1 (12 <sup>th</sup> to 15 <sup>th</sup> July)	42 ± 9 (17 <sup>th</sup> to 20 <sup>th</sup> July)	51 ± 8 (4 <sup>th</sup> to 8 <sup>th</sup> August)
Macronutrients	DIP (nM)	3.7 ± 2.1	3.7 ± 1.0	3.4 ± 0.8	14 ± 0.70
	DOP (nM)	87 ± 7.5	137 ± 39	112	129 ± 29
	DIN (nM)	1.5 ± 1.9	1.66 ± 0.56	3.36 ± 1.0	6.2 ± 0.0
	APA (nM h <sup>-1</sup> )	2.8 ± 0.21	2.86	2.48 ± 0.10	1.15 ± 0.08
Trace metals	dFe (nM)	1.26 ± 0.06	0.53 ± 0.06	0.83 ± 0.00	0.23 ± 0.05
	dZn (nM)	0.25 ± 0.14	0.46 ± 0.09	0.14 ± 0.01	0.04 ± 0.01
	dCo (pM)	11.0	11.1	13.0	13.9
Phytoplankton community	<i>Synechococcus</i> (cells ml <sup>-1</sup> )	3.4 ± 0.55 · 10 <sup>3</sup>	-	-	1.6 ± 0.26 · 10 <sup>3</sup>
	<i>Prochlorococcus</i> (cells ml <sup>-1</sup> )	29 ± 0.37 · 10 <sup>4</sup>	-	-	181 ± 0.37 · 10 <sup>4</sup>
	Chl-a (µg L <sup>-1</sup> )	0.064 ± 0.01	0.055 ± 0.01	0.110 ± 0.06	0.149 ± 0.005

249

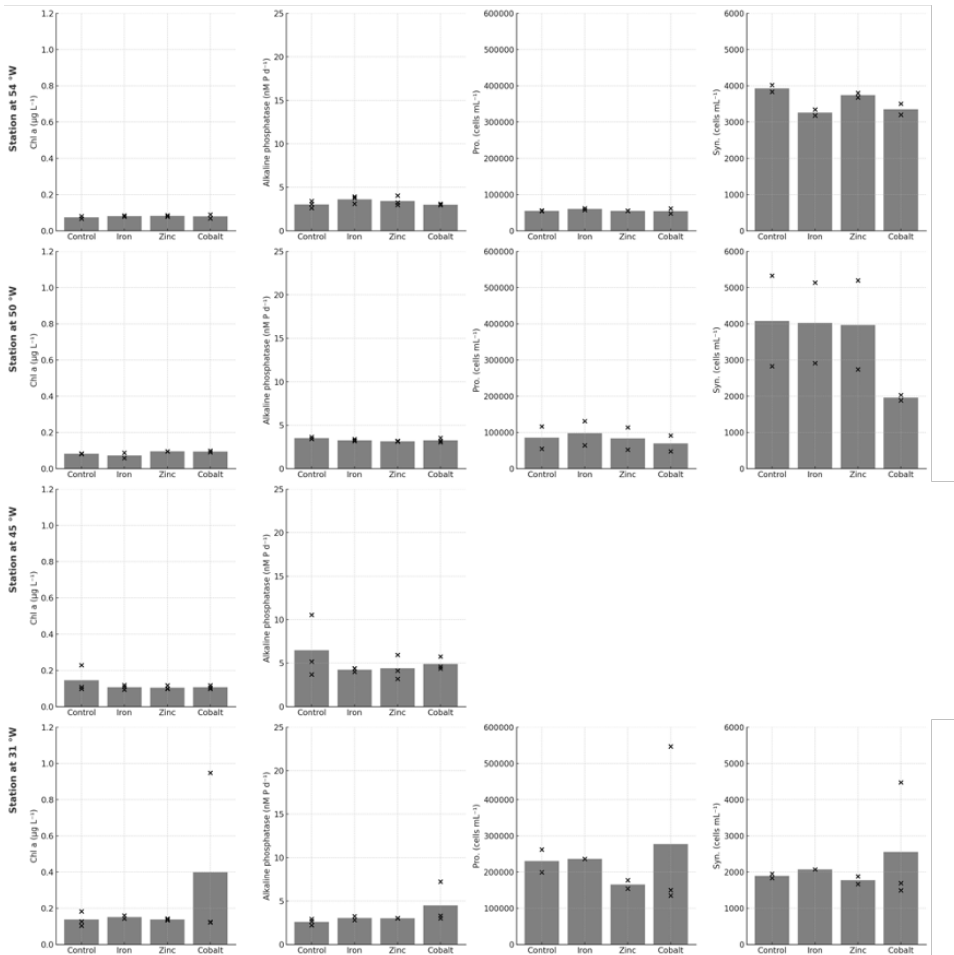
## 250 ‘Traditional’ bioassay responses to the metal-amended bioassays

251 Across the 16 bioassays conducted across the North Atlantic, spanning various metal conditions due  
252 to natural gradients and metal amendments, the bioassays did not result in any observable responses in



253 the conventional parameters such as Chl-*a*, APA, and cell counts for *Prochlorococcus* and  
254 *Synechococcus*. Following a 48-hour incubation period, there were no statistically significant changes,  
255 either positive or negative, compared to the unamended Control (see Fig. 1). This finding remained  
256 consistent in additional experiments conducted at the same location and time as outlined in Mahaffey  
257 et al. (submitted as a companion to this article). At least in part, this may be due to the large  
258 differences between replicate incubation bottles which may have resulted from stochasticity of  
259 sampling the low biomass system of the subtropical North Atlantic. Regardless, the absence of  
260 significant responses in the biogeochemical parameters contrasted notably with the observed  
261 responses in protein data detailed below.

262



263

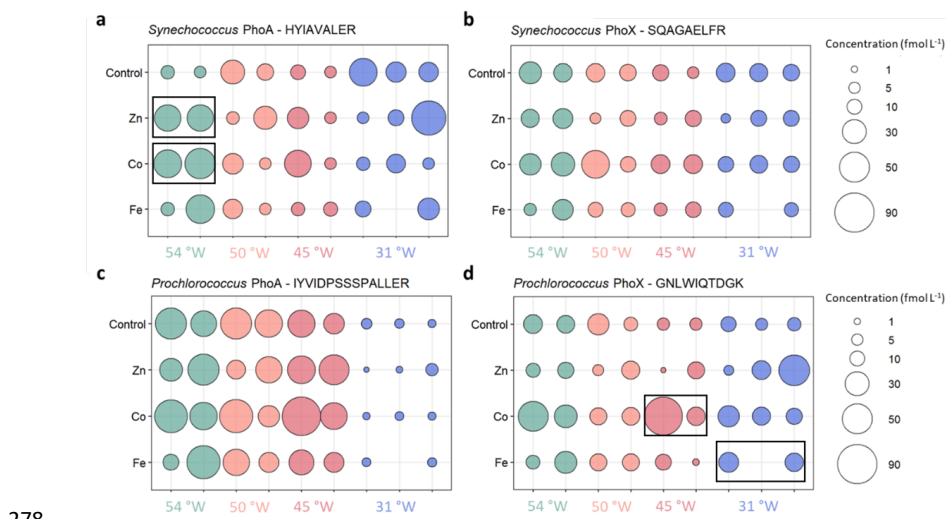
264 *Figure 1* Mean concentrations (grey bars) of the bioassay parameters after the addition of Fe, Zn and Co at the four  
265 stations, specifically (left column) concentrations of chlorophyll *a* ( $\mu\text{g L}^{-1}$ ), (second to left column) rates of alkaline  
phosphatase ( $\text{nM d}^{-1}$ ), (second to right column) *Prochlorococcus* abundance ( $\text{cells mL}^{-1}$ ) and (right column) *Synechococcus*



266 abundance (cells  $mL^{-1}$ ). Dots represent the concentrations of each replicate. Note the data gap for cell counts at the Station  
267 at 45 °W.

## 268 **Absolute concentrations of strain-resolved cyanobacterial alkaline phosphatases**

269 In contrast to the bioassay results, there were clear changes in organism-resolved alkaline phosphatase  
270 concentrations after metal additions. We focused on the enzymes PhoA and PhoX and used peptides  
271 that were specific to one or more strains of either *Prochlorococcus* or *Synechococcus* (Table 2) and  
272 represent a subset of the population of alkaline phosphatase enzymes in the ocean. We note that  
273 marine alkaline phosphatases are found at different subcellular localizations and are also known to be  
274 secreted to the environment (i.e. into the dissolved phase) (Li et al., 1998; Luo et al., 2009). Our  
275 measurements focus on the alkaline phosphatase associated with microbial cells, i.e. the particulate  
276 phase. Coming from an overview of the enzyme concentrations across isoforms, taxa and bioassays,  
277 we will discuss how these compare to the APA assay involving fluorogenic substrates.



278  
279 *Figure 2 Absolute concentrations of the alkaline phosphatases PhoA (left column) and PhoX (right column) of*  
280 *Synechococcus (top) and Prochlorococcus (bottom) in the different metal treatments or the unamended control at the four*  
281 *probed stations. Bubbles of the same colour are replicates of the same treatment and show the concentrations as fmol*  
282 *enzyme per L seawater. Black boxes indicate significant change from Control treatment.*

283 The results of all measured alkaline phosphatase concentrations are shown in Fig. 2 and all  
284 data is compiled in Table S3. *Synechococcus* PhoA and PhoX concentrations in the control treatments  
285 ranged from 6 to 43 fmol L⁻¹ and 6 to 26 fmol L⁻¹, respectively, with no clear cross-basin trend despite  
286 a strong west-to-east decreasing gradient in *Synechococcus* cell abundance (Table 3). Similarly,  
287 *Prochlorococcus* PhoA and PhoX concentrations in the control treatments ranged from 2 to 55 fmol  
288 L⁻¹ and 6 to 23 fmol L⁻¹, respectively, but with elevated PhoA at in the west and the lowest  
289 concentrations at 31 °W, which is opposite to the west-to-east increasing gradient in *Prochlorococcus*



290 cell abundance. This suggests that we observed a gradient in DIP/trace metal nutrient stress for  
291 *Prochlorococcus*, but not for *Synechococcus*.

292 Our measured alkaline phosphatase concentrations were similar, albeit at the lower end, to  
293 concentrations reported for other cyanobacterial enzymes and nutrient regulators from the North  
294 Pacific ( $\sim 10^1$  to  $10^3$  fmol L $^{-1}$ ) (Saito et al., 2014). Interestingly, our alkaline phosphatase  
295 concentrations occurred at the same concentration range as other macronutrient stress indicators  
296 (response regulator protein PhoP, sulfolipid biosynthesis protein SqdB, nitrogen regulatory protein P-  
297 II), all of which did not exceed tens of fmol L $^{-1}$  (Saito et al., 2014). In contrast, concentrations of the  
298 *Prochlorococcus* PstS transporter protein were higher, ranging from 95 to 472 fmol L $^{-1}$  (Table S3).  
299 This is within the concentration range of other cyanobacterial nutrient transporters, such as the urea  
300 transporter UrtA, measured previously (Saito et al., 2014). In mediating nutrient stress, particularly  
301 phosphorus stress, the relative role of transporter proteins (such as PstS) versus other strategically  
302 deployed enzymes like alkaline phosphatase in the oligotrophic specialists *Synechococcus* and  
303 *Prochlorococcus*, represents an interesting avenue for future research.

304 **Metal control on alkaline phosphatases**

305 Our strain-specific, quantitative proteomics approach allowed us to resolve contrasting responses  
306 across the sites. The responses differed with varying phytoplankton species, alkaline phosphatase  
307 form and stimulating metal addition, consistent with differences in the biogeochemical regimes (Table  
308 3). At the iron-rich westernmost station, the *Synechococcus* PhoA concentration increased six- and  
309 seven-fold upon addition of Zn (to  $38 \pm 0.56$  fmol L $^{-1}$ ) and Co (to  $47 \pm 6.8$  fmol L $^{-1}$ ) relative to the  
310 control ( $6.7 \pm 1.5$  fmol L $^{-1}$ ), respectively. At one intermediate Station (45 °W), the *Prochlorococcus*  
311 PhoX concentration increased 8-fold upon addition of Co relative to the control. Notably, a direct  
312 response of alkaline phosphatase to an addition of Co has not been shown in the field before. In  
313 contrast, at the low iron easternmost station, the *Prochlorococcus* PhoX increased over two-fold upon  
314 Fe addition (to  $18 \pm 2.6$  fmol L $^{-1}$ ) relative to the control ( $8.2 \pm 2.4$  fmol L $^{-1}$ ).

315 At least three scenarios are possible to explain the increased alkaline phosphatase  
316 concentrations of *Synechococcus* and *Prochlorococcus* in seawater in these treatments – two  
317 biochemical and one growth driven hypotheses. First, the metal addition may stimulate the production  
318 of the alkaline phosphatase enzyme via a direct or indirect metal regulation on the expression of this  
319 enzyme, as was previously observed for PhoA with Zn additions in *Synechococcus* cultures (Cox and  
320 Saito, 2013). Second, the metal addition may prevent the degradation of the existing alkaline  
321 phosphatases by filling empty metal co-factor sites (Bicknell et al., 1985), with the caveat that PhoA  
322 is likely to be periplasmic and hence unlikely to be actively degraded (Luo et al., 2009). Both  
323 biochemical scenarios allow for increased alkaline phosphatase concentrations at a constant cell



324 abundance. The third explanation is that the alkaline phosphatase concentration increases because the  
325 metal addition stimulates overall cell growth, resulting in higher phosphorus demands and hence more  
326 production of alkaline phosphatase proteins by the cell. This could manifest itself as higher cell  
327 abundances in addition to increased alkaline phosphatase concentration per unit biomass.

328 While the different scenarios are not mutually exclusive, our quantitative proteomic approach  
329 allowed us to discern between biochemical and growth mechanisms by normalising the alkaline  
330 phosphatase concentrations to the total cell counts of *Prochlorococcus* and *Synechococcus*, caveating  
331 that the cell counts are not strain-specific, unlike the peptide-based protein measurements. Cell counts  
332 did not change significantly across these treatments Mahaffey et al. (submitted as a companion to this  
333 article). which means that the trends of increased alkaline phosphatase concentration per L seawater  
334 persisted in bioassays (i.e. +Zn and +Co at 54 °W and +Fe at 31 °W; cell counts do not exist for 45  
335 °W) even when converted to the number of alkaline phosphatase enzymes per cell, indicating  
336 biochemical regulation as opposed to simply growth of the responsible organism. Specifically, the  
337 concentration of *Synechococcus* PhoA increased to  $8418 \pm 673$  enzymes cell<sup>-1</sup> upon Co addition and  
338 to  $6057 \pm 48$  enzymes cell<sup>-1</sup> upon Zn addition relative to  $1025 \pm 257$  enzymes cell<sup>-1</sup> in the control at  
339 54 °W, while the concentration of the *Prochlorococcus* PhoX increased to 59 enzymes cell<sup>-1</sup> upon Fe  
340 addition relative to  $19 \pm 7$  enzymes cell<sup>-1</sup> in the control at 31 °W. Therefore, a direct biochemical  
341 metal control on the alkaline phosphatase concentrations during the bioassays is plausible (i.e. either  
342 of the first two explanations) and adds weight to the hypothesis for the localised metal-phosphorus co-  
343 limitation in the subtropical North Atlantic (Browning et al., 2017; Jakuba, R. Wisniewski et al.,  
344 2008; Mahaffey et al., 2014; Saito et al., 2017; Shaked et al., 2006).

345 These estimates of enzyme copies per cell are potentially underestimates as multiple  
346 *Prochlorococcus* and *Synechococcus* ecotypes co-exist and the alkaline phosphatase peptide  
347 sequences probed here do not encompass all of them (Table 2). Moreover, it is also possible that there  
348 are additional isoforms of alkaline phosphatase present in these organisms that have yet to be  
349 identified. Yet in these marine cyanobacteria, the cellular concentration of alkaline phosphatase was  
350 much higher compared to a measurement in the model bacterium *E. coli*, which contained ~4 PhoA  
351 copies cell<sup>-1</sup> (Wiśniewski and Rakus, 2014). This underscores the ecological demand for alkaline  
352 phosphatases due to the significant depletion of phosphorus in the marine environment. It is yet to be  
353 determined whether the per-cell estimates of alkaline phosphatases presented here are the norm for  
354 marine cyanobacteria, or whether these estimates are exceptionally high due to the prevalence of  
355 phosphorus stress in our study region.

356 While PhoX enzymes are unknown to use Co as a metal co-factor and the response at 45 °W  
357 warrants further investigation, the substitution of Zn with Co in PhoA has been hypothesised  
358 previously based on the distributions of trace metals and phosphate in the Sargasso Sea (Jakuba, R.



359 Wisniewski et al., 2008; Saito et al., 2017). The results from 54 °W support this hypothesis as the  
360 addition of both Zn and Co were associated with almost equal increases of the *Synechococcus* PhoA  
361 concentration relative to the control. It is thought that while Zn is the preferred metal centre for PhoA,  
362 it is possible to substitute Co for Zn in the protein, such as occurs in *Thermotoga maritima*  
363 (Wojciechowski et al., n.d.) *in vivo* and *in vitro* in *E. coli* (Gottesman et al., 1969). Metabolic  
364 substitution capabilities between Zn and Co in carbonic anhydrases have previously been identified in  
365 marine phytoplankton, with similar or slightly reduced growth rates for a range of marine diatoms and  
366 coccolithophores, when Zn was replaced with Co in carbonic anhydrases (Dupont et al., 2006;  
367 Kellogg et al., 2020; Morel et al., 2020; Price and Morel, 1990; Sunda and Huntsman, 1995;  
368 Timmermans et al., 2001; Xu et al., 2007; Yee and Morel, 1996). However, in certain organisms such  
369 as in the coccolithophore *Emiliana huxleyi*, it is possible that Co is the preferred metal co-factor since  
370 the growth rate was higher under replete Co than under replete Zn. One reason could be the co-  
371 evolution of ocean chemistry and cyanobacteria under the Co- and Fe-replete, but Zn-deplete  
372 conditions of the ancient ocean ~2.5 Gyr ago (Dupont et al., 2006; Johnson et al., 2024; Saito et al.,  
373 2003). Another explanation for Co use in alkaline phosphatases may require maintaining low  
374 intracellular availability of Zn to avoid toxicity through inhibition of cobalt insertion by high Zn into  
375 cobalamin (Hawco and Saito, 2018). Supporting this, the cyanobacterium *Synechococcus bacillaris*  
376 and *Prochlorococcus* were found to have absolute Co requirements for growth (Sunda and Huntsman,  
377 1995). Together with these aspects, our insights from the bioassay response at 54 °W merits further  
378 investigations into whether *Synechococcus* can interchange Zn and Co in PhoA, and indeed which  
379 metal is preferred. This would be an important insight for considerations of stoichiometric plasticity  
380 and niche partitioning across the vast Zn- and Co-depleted regions of the ocean, especially where dZn  
381 can become depleted to levels similar or below dCo (Kellogg et al., 2020).

382 Across all bioassays, the addition of Zn did not increase the concentration of any presumably  
383 Fe-dependent PhoX, and the addition of Fe did not increase the concentration of any presumably Zn-  
384 or Co-dependent PhoA. In other words, no significant unexpected responses were observed.  
385 Nevertheless, there are some non-significant trends upon the addition of Co that warrant further study.  
386 For example, the addition of Co increased the putative Fe-containing *Prochlorococcus* PhoX protein  
387 concentration dramatically in one of the replicates at 45 °W and hence, Co could be an efficient metal  
388 co-factor in PhoX (as in the bacterium *Pasteurella multocida* (Wu, Jin-Ru et al., 2007)), or at least,  
389 directly or indirectly stimulate production of PhoX. This contrasts with the results of Kathuria &  
390 Martiny (Kathuria and Martiny, 2011), who hypothesized an enzyme inhibiting role of Co (and Zn;  
391 with Fe untested) for the activity of both *Synechococcus* and *Prochlorococcus* PhoX by replacing  
392  $\text{Ca}^{2+}$  at the active site.

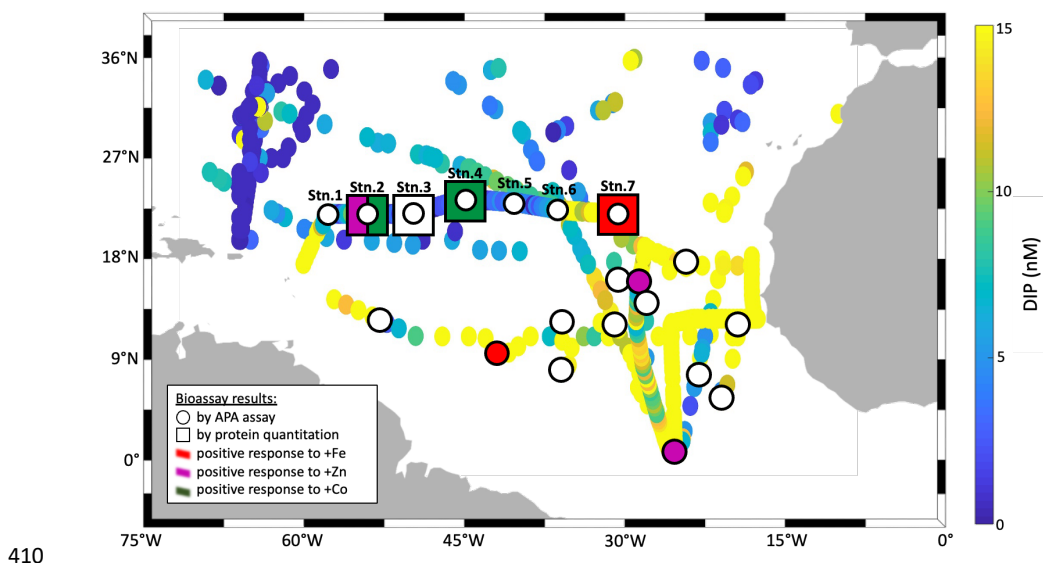
393 Taken together, the results of our bioassays suggest that alkaline phosphatase enzymes are  
394 affected by trace metal concentrations, and that the response to Zn, Co or Fe may be species or strain



395 specific. The metal effects differed between the responsive enzyme type (PhoA versus PhoX) and  
396 phytoplankton species (*Prochlorococcus* versus *Synechococcus*) at contrasting biogeochemical  
397 settings across the basin. It is plausible that the significant changes in protein concentration can result  
398 directly from the metal addition triggering more alkaline phosphatase production per cell. This  
399 demonstrates that the cycling of macronutrients and metals are intermittently linked and that the  
400 nature of that linkage depends on microbial community composition

401 **Alkaline phosphatase abundances in the context of bulk community APA**

402 Alkaline phosphatase activity and phytoplankton biomass (by Chl- $\alpha$  proxy) did not increase  
403 significantly upon the metal additions in the bioassays, neither together with the responses observed in  
404 the absolute enzyme concentrations at 54 °W, 45 °W and 31 °W, nor in any other treatments or  
405 locations (also Mahaffey et al.; submitted). A quantitative explanation for this – and hence a  
406 demonstration of the power of proteomics on the organism level - emerges from estimates of enzyme  
407 abundance-based enzyme rates, where the APA assay covers the entire microbial community (i.e.  
408 everything from bacteria to eukaryotes) but the proteomics measurements are specific to a subset of  
409 *Prochlorococcus* and *Synechococcus*.



411 *Figure 3 Map of the North Atlantic showing surface phosphate concentrations (compiled by Martiny et al., 2019(Martiny et  
412 al., 2019); augmented with data from Browning et al. 2017(Browning et al., 2017)). Overlaid are locations of bioassays,  
413 where the response of APA to metal additions was tested (circles), and of bioassays, where the absolute concentration of the  
414 alkaline phosphatase proteins was measured in response to metal additions (squares). Bioassays of the present study include  
415 longitudinal station labels. The others are from Mahaffey et al. (2014)(Mahaffey et al., 2014) and Browning et al.  
416 (2017)(Browning et al., 2017) as well as from additional bioassays during JC150 Mahaffey et al. (submitted as a companion*



417 to this article). but where no protein measurements were made. Symbols at bioassay locations are coloured in red, purple or  
418 green, if a positive response was observed upon addition of Fe, Zn or Co respectively.

419 The geographically localised changes in the alkaline phosphatase concentrations and the  
420 absence of changes in APA during our bioassays align with the results of Browning et al.(Browning et  
421 al., 2017), where only one in eight experiments showed a metal driven response in APA. Furthermore,  
422 a compilation of bioassay APA measurements from the North Atlantic exposes both the absence and  
423 diversity in metal responses across the basin (Fig. 3). For example, Mahaffey et al.(Mahaffey et al.,  
424 2014) observed a positive response of APA to Zn in the eastern basin, whereas our bioassay results  
425 showed an increase in *Synechococcus* PhoA concentration (but no change in APA) upon Zn addition  
426 in the western basin. While this difference is potentially the result of regional and seasonal drivers,  
427 resolving the apparent ‘patchiness’ of these trends will rely on the better spatial and temporal  
428 coverage of similar studies in the future. One explanation for the presence of the many null responses  
429 across the basin is that organisms effectively re-allocate metals towards use in alkaline phosphatases  
430 when under phosphorus stress. A comparable re-allocation mechanism of cellular Fe between  
431 metalloproteins involved in biological N<sub>2</sub> fixation and photosynthesis has previously been  
432 demonstrated in the diel cycle of *Crocospaera watsonii* (Saito et al., 2011b).

#### 433 **Towards a quantitative, in situ marine metalloproteome of *Synechococcus***

434 An advantage of absolute quantitative measurements over relative proteomics data is the ability to  
435 relate the absolute protein concentrations to other data types, including biological rate measurements  
436 and cellular metal stoichiometry. To this end, the concentrations of the Zn, Co or Fe-dependent  
437 alkaline phosphatases measured in this study naturally lead to two questions: First, how much metal is  
438 allocated as alkaline phosphatase co-factors in the cell, and how does this compare to total cellular  
439 metal content? Second, how does the APA estimated from enzyme abundance compare to assay-based  
440 APA?

441 To address these questions, model calculations were performed. Variables other than the  
442 absolute concentrations of the alkaline phosphatases were either measured concomitantly during the  
443 bioassays, such as cellular metal quotas, cell abundance, APA and DOP concentration, or sourced  
444 from the literature such as strain specific contribution to cell abundance, phosphoester contribution to  
445 the DOP pool, enzyme kinetics parameters and subcellular enzyme localization. We chose to use the  
446 *Synechococcus* PhoA concentrations in the control treatments at 54 °W after 48 h in these calculations  
447 for three reasons: First, cellular metal quotas of *Synechococcus* but not of *Prochlorococcus* were  
448 measured in this treatment, due to limited sampling capacity. Second, enzyme kinetics parameters of  
449 the PhoA rather than PhoX isoform are well documented in the literature(Lazdunski and Lazdunski,  
450 1969). Third, estimates for the contribution of *Synechococcus* strain WH8102 (to which our measured  
451 PhoA is specific) to total *Synechococcus* counts exist from previous studies nearest to 54



452 °W(Ohnemus et al., 2016). A similar reasoning applied to the phosphoester contribution to the DOP  
453 pool. For ease, more detailed explanations, all values, and assumptions are in Tables S1 and S2.

454 Equation 1a approximates the cellular Zn allocation towards the *Synechococcus* PhoA from  
455 the replicate-averaged PhoA concentration in seawater normalised to cell abundance, assuming full  
456 metalation of the enzyme with four metal ions per dimer(Coleman, 1992). The cell abundance is a  
457 function of *Synechococcus* cell counts and the fractional abundance of strain WH8102, to which the  
458 measured PhoA is specific. Equation 1b expresses the results of Equation 1a as a fraction of the total  
459 cellular Zn content.

460 Allocated  $Zn_{PhoA}$  = metalated co-factors<sub>PhoA</sub> \* PhoA<sub>SW</sub> / (Syn. abundance \* WH8102 fraction) (1a)

461 Fractional allocated  $Zn_{PhoA}$  =  $Zn_{PhoA}$  /  $Zn_{total\ cell}$ . (1b)

462 The amount of metal allocated to PhoA in *Synechococcus* is 3,054 atoms cell<sup>-1</sup>. This translates  
463 to a maximum fractional contribution towards the total cellular Zn content of 0.66 % after dividing by  
464 cellular Zn measured using SXRF (Table S1). If the co-factor in PhoA is assumed to be occupied by  
465 Co<sup>2+</sup> instead of Zn<sup>2+</sup>, the fractional contribution to the cellular Co content is 38 %, due to the lower  
466 total cellular Co content of *Synechococcus* compared to Zn (Table S1). It is possible that the active  
467 sites of PhoA are occupied by a mixture of Zn and Co, incompletely metalated, or under competition  
468 by metals other than Zn or Co. Nevertheless, these low fractional contributions of PhoA-allocated Zn  
469 appear biochemically reasonable, as the majority of Zn in *Synechococcus* appears to be stored in  
470 metallothioneins to maintain Zn homeostasis and potentially supply alkaline phosphatases with Zn as  
471 needed (Cox and Saito, 2013; Mikhaylina et al., 2022). However, our bioassay results also suggest Zn  
472 may not be the preferred co-factor in *Synechococcus* PhoA: The larger response of this enzyme to Co  
473 additions at 54 °W suggests the effective substitution of or even preference for Co (Fig. 2). This  
474 would align with evolutionary arguments (see ‘Metal control on alkaline phosphatases’) and imply  
475 that PhoA is a potential major sink of cellular Co. This would also imply that *Synechococcus* growth  
476 may be sensitive towards Co-phosphorus co-limitation in the oligotrophic ocean.

477 Equation 2a approximates the *Synechococcus* PhoA-abundance based hydrolysis rate as a  
478 function of the PhoA concentration (converting molarity units to grams using its molecular weight),  
479 phosphoester substrate concentration, and Michaelis-Menten kinetics parameters  $V_{max}$  and  $K_m$ , the  
480 maximum reaction rate and half-saturation constant, respectively, derived from an *E. coli* homologue  
481 of PhoA (Table S2). Equation 2b expresses the results of Equation 2a as a fraction of the ‘total APA’,  
482 a function of the measured MUF-P assay-based APA with a correction applied for the subcellular  
483 localisation of marine alkaline phosphatases, of which only the periplasmic-outwards fraction (~20 to  
484 80 %) is detectable via the MUF-P assay. In other words, the calculated ‘total APA’ accounts for both  
485 the dissolved and particulate activity. Details on made assumptions are in the supplement (Table S2).



486  $\text{Rate}_{\text{PhoA}} = \text{PhoA}_{\text{SW}} * \text{molecular weight} * V_{\text{max}} * \text{substrate} / (\text{substrate} + K_m)$  (2a)

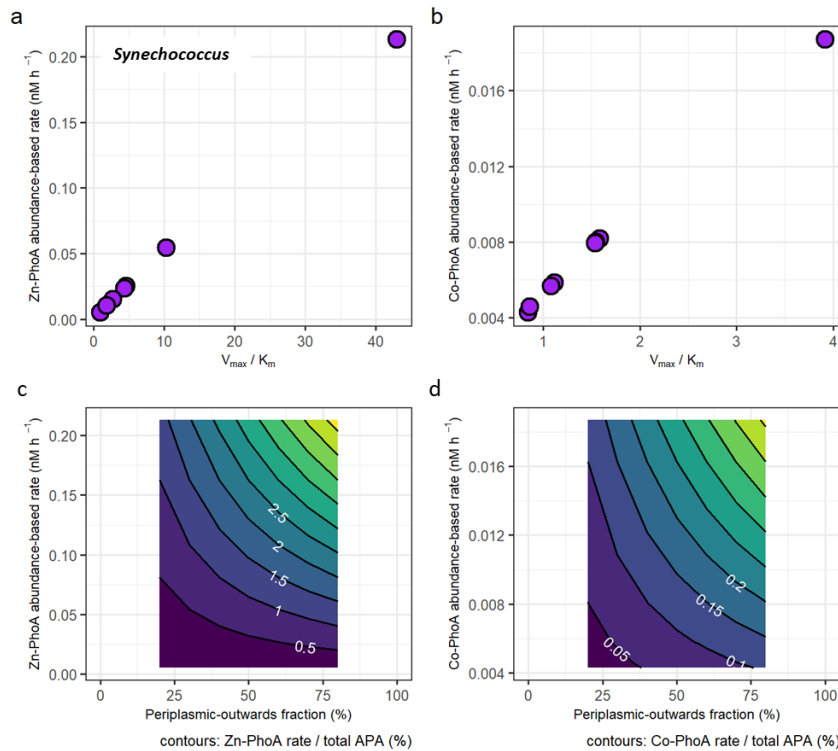
487 where substrate = DOP \* phosphoester fraction

488 Fractional Rate<sub>PhoA</sub> = Rate<sub>PhoA</sub> \* periplasmic-outwards fraction / assayed APA (2b)

489 The protein abundance-based rates range from 0.00517 nM h<sup>-1</sup> to 0.213 nM h<sup>-1</sup> for the Zn-  
490 dependent *Synechococcus* PhoA and from 0.00428 nM h<sup>-1</sup> to 0.0187 nM h<sup>-1</sup> for the Co-dependent  
491 PhoA (Fig. 4a and b), using the *E. coli* kinetics parameters for each metal that are slower under Co  
492 coordination. In terms of fractional contributions to total APA, the rate estimates translate to  
493 maximally 5.2 % for Zn-PhoA and 0.46 % for the Co-PhoA. Regardless of the choice of enzyme  
494 kinetics, it appeared that *Synechococcus* PhoA contributed a small component to the total APA in our  
495 bioassays. This concurs with the observed increase in concentration of *Synechococcus* PhoA upon  
496 metal addition versus the null response in APA. Applying the same calculation and kinetics  
497 parameters for the case of the *Prochlorococcus* PhoA yields abundance-based rates between 0.0347  
498 nM h<sup>-1</sup> and 1.42 nM h<sup>-1</sup> for the Zn-PhoA and between 0.0287 nM h<sup>-1</sup> and 0.125 nM h<sup>-1</sup> for the Co-  
499 PhoA, which translate to maximal contributions to the total APA of 35 % and 3.1 %, respectively.  
500 These higher rates and fractional contributions compared to the *Synechococcus* PhoA are due to the  
501 higher concentrations of the *Prochlorococcus* PhoA than the *Synechococcus* PhoA in the chosen  
502 samples. The taxon-specific alkaline phosphatase concentrations illustrate the challenge of  
503 interpreting bulk enzyme activities when the functional enzyme class is produced by many biological  
504 taxa (cyanobacteria, heterotrophic bacteria, diatoms etc.). In essence, the different bioassay responses



505 shown here demonstrate the need to further develop a “meta-biochemistry” capability to understand  
506 biogeochemical reactions at the mechanistic level.



507

508 *Figure 4 (a) Protein abundance-based APA estimates of Synechococcus Zn-dependent PhoA as a function of different*  
509 *enzyme kinetic parameters  $V_{max}$  and  $K_m$ . (b) Same as (a), but with enzyme parameters for the less efficient Co-dependent*  
510 *PhoA. (see Table S2). (c) The fraction of the Zn-PhoA abundance-based APA from (a) over the total APA. (d) Same as (c)*  
511 *but using the Co-PhoA rates from (b). Note the scale difference between (a,c) and (b,d).*

512 The enzyme-based rates calculated here may be below that of bulk activity (APA assay) due  
513 to our focus on a few species within the particulate phase of the enzyme. Alkaline phosphatase is  
514 known to be more abundant in the dissolved phase, for example as much as 72% of the APA was  
515 observed in Red Sea samples to be in the dissolved phase(Li et al., 1998). Moreover, the periplasmic  
516 location of alkaline phosphatase has been observed to result in loss during preservation. In a  
517 preservation study, PhoA was notably the protein with the lowest recovery in *Synechococcus*  
518 WH8102 after a month in storage compared to  $101\% \pm 27\%$  for the fifty most abundant proteins(Saito  
519 et al., 2011a). The combination of multiple abundant and rare microbial sources of alkaline  
520 phosphatases together contribute to the particulate, and when secreted or lost, dissolved reservoirs that  
521 make up the bulk APA.

522 **Conclusions**



523 This study performs taxon-specific alkaline phosphatase isoform analysis via absolute quantitative  
524 proteomics on *Prochlorococcus* and *Synechococcus*, coupled to enzyme bioassays. This approach  
525 supports the use of Zn, Co and Fe in alkaline phosphatases in the natural oceanic environment, but  
526 also adds complexity to our understanding of how these enzymes are regulated in a biogeochemical  
527 context. Our mechanistic perspective revealed that these two highly abundant microbes are only  
528 minor contributors to bulk APA, which carries important implications for the interpretation of the  
529 widely used fluorescent APA assay. Additionally, within this picocyanobacterial class, we observed  
530 heterogeneous responses of the alkaline phosphatase enzymes depending on the protein, taxonomy,  
531 biogeochemical context, and treatment. This indicates that there is significant biological diversity in  
532 the responses of individual marine organisms to experimental treatments that can be resolved by  
533 combining enzyme assay measurements with quantitative proteomics. Our results indicate a need for  
534 biochemical characterisation of key marine alkaline phosphatases, particularly with regards to their  
535 kinetics and metal co-factors as highlighted by the potential importance of Co as a metal co-factor in  
536 PhoA and possibly PhoX. Future efforts to understand the biochemical properties of marine microbes  
537 will benefit the connected interpretation of molecular, enzymatic, and biogeochemical assays, and in  
538 turn our understanding of nutrient cycling in the ocean system.

### 539 Acknowledgements

540 The authors would like to thank the captain and crew of the *R.R.S. James Cook* during cruise JC150,  
541 as well as all the scientific party members, who helped to conduct the bioassays. The authors would  
542 also like to thank Alastair Lough and Clément Demasy for the dCo measurements, and Julie Robidart  
543 and Rosalind Rickaby for fruitful discussions on this manuscript. This research was supported by the  
544 National Environmental Research Council (UK) under grants NE/N001125/1 to MCL and  
545 NE/N001079/1 to CM, by the National Science Foundation (USA) under grant OCE1829819 to BST,  
546 OCE1924554, OCE1850719 and NIH R01GM135709 to MAS, and by the Graduate School of the  
547 National Oceanography Centre Southampton (UK) to KK. The writing process was also supported by  
548 the Simons Foundation under award 723552 to KK and by the USC Dornsife College of Arts and  
549 Sciences to NAH.

550 **Author contributions:** NAH and KK wrote the initial manuscript draft. NAH and KK performed the  
551 proteomics analysis with help from MM and MAS. KK, NAH, NJW, CD, CM, MCL performed the  
552 experiments at sea. BST and ELM conducted the cell quota measurements. MCL, CM, AT and MAS  
553 led the research campaign. All authors commented on the manuscript.

554 **Competing interests:** The authors declare no competing interests.

555 **Data Availability:** Source data for all main and supplementary figures are provided in the  
556 supplement. The mass spectrometry proteomics data have been deposited to the ProteomeXchange  
557 Consortium via the PRIDE [1] partner repository with the dataset identifier PXD053717.



558 **References**

- 559 Bicknell, R., Schaeffer, A., Auld, D. S., Riordan, J. F., Monnanni, R., and Bertini, I.: Protease  
560 susceptibility of zinc - and APO-carboxypeptidase A, *Biochemical and Biophysical Research  
561 Communications*, 133, 787–793, [https://doi.org/10.1016/0006-291X\(85\)90973-8](https://doi.org/10.1016/0006-291X(85)90973-8), 1985.
- 562 Browning, T. J., Achterberg, E. P., Yong, J. C., Rapp, I., Utermann, C., Engel, A., and Moore, C. M.:  
563 Iron limitation of microbial phosphorus acquisition in the tropical North Atlantic, *Nature  
564 Communications*, 8, 1–7, <https://doi.org/10.1038/ncomms15465>, 2017.
- 565 Carvalho, P. C., Fischer, J. S. G., Chen, E. I., Yates, J. R., and Barbosa, V. C.: PatternLab for  
566 proteomics: A tool for differential shotgun proteomics, *BMC Bioinformatics*, 9, 1–14,  
567 <https://doi.org/10.1186/1471-2105-9-316>, 2008.
- 568 Coleman, J. E.: Structure and mechanism of alkaline phosphatase, *Annu Rev Biophys Biomol Struct*,  
569 21, 441–483, <https://doi.org/10.1146/annurev.bb.21.060192.002301>, 1992.
- 570 Cox, A. D. and Saito, M. A.: Proteomic responses of oceanic *Synechococcus* WH8102 to phosphate  
571 and zinc scarcity and cadmium additions, *Frontiers in Microbiology*, 4, 1–17,  
572 <https://doi.org/10.3389/fmicb.2013.00387>, 2013.
- 573 Davis, C., Lohan, M. C., Tuerena, R., Cerdan-Garcia, E., Woodward, E. M. S., Tagliabue, A., and  
574 Mahaffey, C.: Diurnal variability in alkaline phosphatase activity and the potential role of  
575 zooplankton, *Limnology and Oceanography Letters*, 4, 71–78, <https://doi.org/10.1002/lol2.10104>,  
576 2019.
- 577 Duhamel, S., Dyhrman, S. T., and Karl, D. M.: Alkaline phosphatase activity and regulation in the  
578 North Pacific Subtropical Gyre, *Limnology and Oceanography*, 55, 1414–1425,  
579 <https://doi.org/10.4319/lo.2010.55.3.1414>, 2010.
- 580 Dupont, C. L., Yang, S., Palenik, B., and Bourne, P. E.: Modern proteomes contain putative imprints  
581 of ancient shifts in trace metal geochemistry., *Proceedings of the National Academy of Sciences of  
582 the United States of America*, 103, 17822–7, <https://doi.org/10.1073/pnas.0605798103>, 2006.
- 583 Dyhrman, S. T. and Ruttenberg, K. C.: Presence and regulation of alkaline phosphatase activity in  
584 eukaryotic phytoplankton from the coastal ocean: Implications for dissolved organic phosphorus  
585 remineralization, *Limnology and Oceanography*, 51, 1381–1390,  
586 <https://doi.org/10.4319/lo.2006.51.3.1381>, 2006.
- 587 Gottesman, M., Simpson, R. T., and Vallee, B. L.: Kinetic properties of cobalt alkaline phosphatase,  
588 *Biochemistry*, 8, 3776–3783, <https://doi.org/10.1021/bi00837a043>, 1969.
- 589 Hawco, N. J. and Saito, M. A.: Competitive inhibition of cobalt uptake by zinc and manganese in a  
590 pacific Prochlorococcus strain: Insights into metal homeostasis in a streamlined oligotrophic  
591 cyanobacterium, *Limnology and Oceanography*, 63, 2229–2249, <https://doi.org/10.1002/lno.10935>,  
592 2018.
- 593 Held, N. A., Webb, E. A., McIlvin, M. M., Hutchins, D. A., Cohen, N. R., Moran, D. M., Kunde, K.,  
594 Lohan, M. C., Mahaffey, C. M., Woodward, E. M. S., and Saito, M. A.: Co-occurrence of Fe and P  
595 stress in natural populations of the marine diazotroph *Trichodesmium*, *Biogeosciences*, 17, 2537–  
596 2551, <https://doi.org/10.5194/bg-2019-493>, 2020.



- 597 Hoffmann, L. J., Breitbarth, E., Boyd, P. W., and Hunter, K. A.: Influence of ocean warming and  
598 acidification on trace metal biogeochemistry, *Marine Ecology Progress Series*, 470, 191–205,  
599 <https://doi.org/10.3354/meps10082>, 2012.
- 600 Jakuba, R., Wisniewski, Moffett, J. W., and Dyhrman, S. T.: Evidence for the linked biogeochemical  
601 cycling of zinc, cobalt, and phosphorus in the western North Atlantic Ocean, *Global Biogeochemical  
602 Cycles*, 22, 2008.
- 603 Johnson, J. E., Present, T. M., and Valentine, J. S.: Iron: Life's primeval transition metal, *Proceedings  
604 of the National Academy of Sciences*, 121, e2318692121, <https://doi.org/10.1073/pnas.2318692121>,  
605 2024.
- 606 Kathuria, S. and Martiny, A. C.: Prevalence of a calcium-based alkaline phosphatase associated with  
607 the marine cyanobacterium *Prochlorococcus* and other ocean bacteria, *Environ Microbiol*, 13, 74–83,  
608 <https://doi.org/10.1111/j.1462-2920.2010.02310.x>, 2011.
- 609 Kellogg, R. M., McIlvin, M. R., Vedamati, J., Twining, B. S., Moffett, J. W., Marchetti, A., Moran,  
610 D. M., and Saito, M. A.: Efficient zinc/cobalt inter-replacement in northeast Pacific diatoms and  
611 relationship to high surface dissolved Co : Zn ratios, *Limnology and Oceanography*, 65, 2557–2582,  
612 <https://doi.org/10.1002/lo.11471>, 2020.
- 613 Kim, I.-N., Lee, K., Gruber, N., Karl, D. M., Bullister, J. L., Yang, S., and Kim, T.-W.: Chemical  
614 oceanography. Increasing anthropogenic nitrogen in the North Pacific Ocean, *Science*, 346, 1102–  
615 1106, <https://doi.org/10.1126/science.1258396>, 2014.
- 616 Kolowith, L. C., Ingall, E. D., and Benner, R.: Composition and cycling of marine organic  
617 phosphorus, *Limnology & Oceanography*, 46, 309–320, <https://doi.org/10.4319/lo.2001.46.2.0309>,  
618 2001.
- 619 Kunde, K., Wyatt, N. J., González-Santana, D., Tagliabue, A., Mahaffey, C., and Lohan, M. C.: Iron  
620 Distribution in the Subtropical North Atlantic: The Pivotal Role of Colloidal Iron, *Global  
621 Biogeochemical Cycles*, 2019GB006326, <https://doi.org/10.1029/2019GB006326>, 2019.
- 622 Lazdunski, C. and Lazdunski, M.: Zn<sup>2+</sup> and Co<sup>2+</sup>-alkaline phosphatases of *E. coli*. A comparative  
623 kinetic study, *Eur J Biochem*, 7, 294–300, <https://doi.org/10.1111/j.1432-1033.1969.tb19606.x>, 1969.
- 624 Li, H., Veldhuis, M., and Post, A.: Alkaline phosphatase activities among planktonic communities in  
625 the northern Red Sea, *Mar. Ecol. Prog. Ser.*, 173, 107–115, <https://doi.org/10.3354/meps173107>,  
626 1998.
- 627 Lohan, M. C. and Tagliabue, A.: Oceanic Micronutrients: Trace Metals that are Essential for Marine  
628 Life, *Elements*, 14, 385–390, <https://doi.org/10.2138/gselements.14.6.385>, 2018.
- 629 Lomas, M. W., Burke, A. L., Lomas, D. A., Bell, D. W., Shen, C., Dyhrman, S. T., and Ammerman,  
630 J. W.: Sargasso Sea phosphorus biogeochemistry: an important role for dissolved organic phosphorus  
631 (DOP), *Biogeosciences*, 7, 695–710, <https://doi.org/10.5194/bg-7-695-2010>, 2010.
- 632 Lu, X. and Zhu, H.: Tube-Gel Digestion: A Novel Proteomic Approach for High Throughput Analysis  
633 of Membrane Proteins, *Mol Cell Proteomics*, 4, 1948–1958, <https://doi.org/10.1074/mcp.M500138MCP200>, 2005.
- 635 Lundgren, D. H., Hwang, S. I., Wu, L., and Han, D. K.: Role of spectral counting in quantitative  
636 proteomics, *Expert Review of Proteomics*, 7, 39–53, <https://doi.org/10.1586/epr.09.69>, 2010.



- 637 Luo, H., Benner, R., Long, R. A., and Hu, J.: Subcellular localization of marine bacterial alkaline  
638 phosphatases, *Proceedings of the National Academy of Sciences of the United States of America*, 106,  
639 21219–21223, <https://doi.org/10.1073/pnas.0907586106>, 2009.
- 640 MacLean, B., Tomazela, D. M., Shulman, N., Chambers, M., Finney, G. L., Frewen, B., Kern, R.,  
641 Tabb, D. L., Liebler, D. C., and MacCoss, M. J.: Skyline: an open source document editor for creating  
642 and analyzing targeted proteomics experiments, *Bioinformatics*, 26, 966–968,  
643 <https://doi.org/10.1093/bioinformatics/btq054>, 2010.
- 644 Mahaffey, C., Reynolds, S., Davis, C. E., Lohan, M. C., and Lomas, M. W.: Alkaline phosphatase  
645 activity in the subtropical ocean: insights from nutrient, dust and trace metal addition experiments,  
646 *Frontiers in Marine Science*, 1, 1–13, <https://doi.org/10.3389/fmars.2014.00073>, 2014.
- 647 Martiny, A. C., Coleman, M. L., and Chisholm, S. W.: Phosphate acquisition genes in  
648 Prochlorococcus ecotypes: Evidence for genome-wide adaptation, *Proceedings of the National  
649 Academy of Sciences*, 103, 12552–12557, <https://doi.org/10.1073/pnas.0601301103>, 2006.
- 650 Martiny, A. C., Lomas, M. W., Fu, W., Boyd, P. W., Chen, Y. L., Cutter, G. A., Ellwood, M. J.,  
651 Furuya, K., Hashihama, F., Kanda, J., Karl, D. M., Kodama, T., Li, Q. P., Ma, J., Moutin, T.,  
652 Woodward, E. M. S., and Moore, J. K.: Biogeochemical controls of surface ocean phosphate, *Science  
653 Advances*, 5, eaax0341, <https://doi.org/10.1126/sciadv.aax0341>, 2019.
- 654 Mather, R., Reynolds, S., Wolff, G., Williams, R., Torres-Valdés, S., Woodward, E., Angela, L., Pan,  
655 X., Sanders, R., and Achterberg, E.: Phosphorus cycling in the North and South Atlantic Ocean  
656 subtropical gyres, *Nature Geoscience*, 1, 439–443, <https://doi.org/10.1038/ngeo232>, 2008.
- 657 Mikhaylina, A., Scott, L., Scanlan, D. J., and Blindauer, C. A.: A metallothionein from an open ocean  
658 cyanobacterium removes zinc from the sensor protein controlling its transcription, *J Inorg Biochem*,  
659 230, 111755, <https://doi.org/10.1016/j.jinorgbio.2022.111755>, 2022.
- 660 Moore, C. M., Mills, M. M., Arrigo, K. R., Berman-Frank, I., Bopp, L., Boyd, P. W., Galbraith, E. D.,  
661 Geider, R. J., Guieu, C., Jaccard, S. L., Jickells, T. D., Roche, J. L., Lenton, T. M., Mahowald, N. M.,  
662 Marañón, E., Marinov, I., Moore, J. K., Nakatsuka, T., Oschlies, A., Saito, M. A., Thingstad, T. F.,  
663 Tsuda, A., and Ulloa, O.: Processes and Patterns of Oceanic Nutrient Limitation, *Nat Geoscience*, 6,  
664 701–710, 2013.
- 665 Morel, F. M. M., Lam, P. J., and Saito, M. A.: Trace Metal Substitution in Marine Phytoplankton,  
666 Annual Review of Earth and Planetary Sciences, 48, 491–517, <https://doi.org/10.1146/annurev-earth-053018-060108>, 2020.
- 668 Ohnemus, D. C., Rauschenberg, S., Krause, J. W., Brzezinski, M. A., Collier, J. L., Geraci-Yee, S.,  
669 Baines, S. B., and Twining, B. S.: Silicon content of individual cells of *Synechococcus* from the North  
670 Atlantic Ocean, *Marine Chemistry*, 187, 16–24, <https://doi.org/10.1016/j.marchem.2016.10.003>, 2016.
- 671 Price, N. M. and Morel, F. M. M.: Cadmium and cobalt substitution for zinc in a marine diatom,  
672 *Nature*, 344, 658–660, <https://doi.org/10.1038/344658a0>, 1990.
- 673 Saito, M., Alexander, H., Benway, H., Boyd, P., Gledhill, M., Kujawinski, E., Levine, N., Maheigan,  
674 M., Marchetti, A., Obernosterer, I., Santoro, A., Shi, D., Suzuki, K., Tagliabue, A., Twining, B., and  
675 Maldonado, M.: The Dawn of the BioGeoSCAPES Program: Ocean Metabolism and Nutrient Cycles  
676 on a Changing Planet, *Oceanog*, 37, <https://doi.org/10.5670/oceanog.2024.417>, 2024.
- 677 Saito, M. A., Sigman, D. M., and Morel, F. M. M.: The bioinorganic chemistry of the ancient ocean:  
678 The co-evolution of cyanobacterial metal requirements and biogeochemical cycles at the Archean-



- 679 Proterozoic boundary?, *Inorganica Chimica Acta*, 356, 308–318, [https://doi.org/10.1016/S0020-1693\(03\)00442-0](https://doi.org/10.1016/S0020-1693(03)00442-0), 2003.
- 680
- 681 Saito, M. A., Bulygin, V. V., Moran, D. M., Taylor, C., and Scholin, C.: Examination of Microbial  
682 Proteome Preservation Techniques Applicable to Autonomous Environmental Sample Collection,  
683 *Front Microbiol*, 2, 215, <https://doi.org/10.3389/fmicb.2011.00215>, 2011a.
- 684 Saito, M. A., Bertrand, E. M., Dutkiewicz, S., Bulygin, V. V., Moran, D. M., Monteiro, F. M.,  
685 Follows, M. J., Valois, F. W., and Waterbury, J. B.: Iron conservation by reduction of metalloenzyme  
686 inventories in the marine diazotroph *Crocospaera watsonii*, *Proceedings of the National Academy of  
687 Sciences of the United States of America*, 108, 2184–9, <https://doi.org/10.1073/pnas.1006943108>,  
688 2011b.
- 689 Saito, M. A., McIlvin, M. R., Moran, D. M., Goepfert, T. J., DiTullio, G. R., Post, A. F., and  
690 Lamborg, C. H.: Multiple nutrient stresses at intersecting Pacific Ocean biomes detected by protein  
691 biomarkers., *Science (New York, N.Y.)*, 345, 1173–7, <https://doi.org/10.1126/science.1256450>, 2014.
- 692 Saito, M. a., Dorsk, A., Post, A. F., McIlvin, M. R., Rappé, M. S., DiTullio, G. R., and Moran, D. M.:  
693 Needles in the blue sea: Sub-species specificity in targeted protein biomarker analyses within the vast  
694 oceanic microbial metaproteome, *Proteomics*, <https://doi.org/10.1002/pmic.201400630>, 2015.
- 695 Saito, M. A., Noble, A. E., Hawco, N., Twining, B. S., Ohnemus, D. C., John, S. G., Lam, P.,  
696 Conway, T. M., Johnson, R., Moran, D., and McIlvin, M.: The acceleration of dissolved cobalt's  
697 ecological stoichiometry due to biological uptake, remineralization, and scavenging in the Atlantic  
698 Ocean, *Biogeosciences*, 14, 4637–4662, <https://doi.org/10.5194/bg-14-4637-2017>, 2017.
- 699 Saito, M. A., McIlvin, M. R., Moran, D. M., Santoro, A. E., Dupont, C. L., Rafter, P. A., Saunders, J.  
700 K., Kaul, D., Lamborg, C. H., Westley, M., Valois, F., and Waterbury, J. B.: Abundant nitrite-  
701 oxidizing metalloenzymes in the mesopelagic zone of the tropical Pacific Ocean, *Nature Geoscience*,  
702 13, <https://doi.org/10.1038/s41561-020-0565-6>, 2020.
- 703 Santos-Benedit, F.: The Pho regulon: a huge regulatory network in bacteria, *Frontiers in Microbiology*,  
704 6, 1–14, <https://doi.org/10.3389/fmicb.2015.00402>, 2015.
- 705 Saunders, J. K., Gaylord, D. A., Held, N. A., Symmonds, N., Dupont, C., Shepherd, A., Kinkade, D.  
706 B., and Saito, M. A.: METATRYP v 2.0: Metaproteomic Least Common Ancestor Analysis for  
707 Taxonomic Inference Using Specialized Sequence Assemblies - Standalone Software and Web  
708 Servers for Marine Microorganisms and Coronaviruses, *Journal of Proteome Research*,  
709 <https://doi.org/10.1021/acs.jproteome.0c00385>, 2020.
- 710 Scanlan, D. J., Mann, N. H., and Carr, N. G.: The response of the picoplanktonic marine  
711 cyanobacterium *Synechococcus* species WH7803 to phosphate starvation involves a protein  
712 homologous to the periplasmic phosphate-binding protein of *Escherichia coli*, *Mol Microbiol*, 10,  
713 181–191, <https://doi.org/10.1111/j.1365-2958.1993.tb00914.x>, 1993.
- 714 Shaked, Y., Xu, Y., Leblanc, K., and Morel, F. M. M.: Zinc availability and alkaline phosphatase  
715 activity in *Emiliania huxleyi*: Implications for Zn-P co-limitation in the ocean, *Limnology and  
716 Oceanography*, 51, 299–309, <https://doi.org/10.4319/lo.2006.51.1.0299>, 2006.
- 717 Sunda, W. G. and Huntsman, S. A.: Cobalt and zinc interreplacement in marine phytoplankton:  
718 Biological and geochemical implications, *Limnology and Oceanography*, 40, 1404–1417,  
719 <https://doi.org/10.4319/lo.1995.40.8.1404>, 1995.
- 720 Timmermans, K. R., Snoek, J., Gerringa, L. J. A., Zondervan, I., and de Baar, H. J. W.: Not all  
721 eukaryotic algae can replace zinc with cobalt: *Chaetoceros calcitrans* (Bacillariophyceae) versus



- 722 Emiliania huxleyi (Prymnesiophyceae), Limnology and Oceanography, 46, 699–703,  
723 <https://doi.org/10.4319/lo.2001.46.3.0699>, 2001.
- 724 Wiśniewski, J. R. and Rakus, D.: Quantitative analysis of the Escherichia coli proteome, Data Brief,  
725 1, 7–11, <https://doi.org/10.1016/j.dib.2014.08.004>, 2014.
- 726 Wojciechowski, C. L., Cardia, J. P., and Kantrowitz, E. R.: Alkaline phosphatase from the  
727 hyperthermophilic bacterium *T. maritima* requires cobalt for activity - Wojciechowski - 2002 -  
728 Protein Science - Wiley Online Library, Protein Science, 11, 903–911, n.d.
- 729 Wu, Jin-Ru, Shien, Jui-Hung, Shieh, Happy K., Hu, Chung-Chi, Gong, Shuen-Rong, Chen, Ling-Yun,  
730 and Chang, Poa-Chun: Cloning of the gene and characterization of the enzymatic properties of the  
731 monomeric alkaline phosphatase (PhoX) from *Pasteurella multocida* strain X-73, FEMS Microbiology  
732 Letters, 267, 2007.
- 733 Wurl, O., Zimmer, L., and Cutter, G. A.: Arsenic and phosphorus biogeochemistry in the ocean:  
734 Arsenic species as proxies for P-limitation, Limnology and Oceanography, 58, 729–740,  
735 <https://doi.org/10.4319/lo.2013.58.2.02729>, 2013.
- 736 Xu, Y., Tang, D., Shaked, Y., and Morel, F. M. M.: Zinc, cadmium, and cobalt interreplacement and  
737 relative use efficiencies in the coccolithophore *Emiliania huxleyi*, Limnology and Oceanography, 52,  
738 2294–2305, <https://doi.org/10.4319/lo.2007.52.5.2294>, 2007.
- 739 Yee, D. and Morel, F. M. M.: In vivo substitution of zinc by cobalt in carbonic anhydrase of a marine  
740 diatom, Limnology and Oceanography, 41, 573–577, <https://doi.org/10.4319/lo.1996.41.3.0573>, 1996.
- 741 Yong, S. C., Roversi, P., Lillington, J., Rodriguez, F., Krehenbrink, M., Zeldin, O. B., Garman, E. F.,  
742 Lea, S. M., and Berks, B. C.: A complex iron-calcium cofactor catalyzing phosphotransfer chemistry.,  
743 Science (New York, N.Y.), 345, 1170–3, <https://doi.org/10.1126/science.1254237>, 2014.
- 744 Young, C. L. and Ingall, E. D.: Marine Dissolved Organic Phosphorus Composition: Insights from  
745 Samples Recovered Using Combined Electrodialysis/Reverse Osmosis, Aquat Geochem, 16, 563–  
746 574, <https://doi.org/10.1007/s10498-009-9087-y>, 2010.
- 747 Zhang, B., VerBerkmoes, N. C., Langston, M. A., Uberbacher, E., Hettich, R. L., and Samatova, N.  
748 F.: Detecting differential and correlated protein expression in label-free shotgun proteomics, Journal  
749 of Proteome Research, 5, 2909–2918, <https://doi.org/10.1021/pr0600273>, 2006.